Neuron, Volume *98*

Supplemental Information

Transformation of a Spatial Map across the Hippocampal-Lateral Septal Circuit

David Tingley and György Buzsáki

Supplemental Information

Figure S1. Technical details: histology, cluster quality, and behavior. Related to Figures 1 and 2. **(A)** Diagrams of the silicon probe locations and supporting histology are given for each animal. Red triangles indicate track localization for each image. All images are sorted anterior-to-posterior in the left-to-right direction. **(B)** *Upper:* Average waveforms across 8 electrodes of a single silicon shank for 14 simultaneously recorded LS neurons. *Lower:* Auto-correlograms for the same 14 neurons are shown as the colored bar plots. Colors match the waveforms in upper panel. Cross-correlograms between each possible cell pair are shown in the white bar plots. X-axis bins are 0.5 ms, and each y-axis is normalized to the maximum count. **(C)** *Upper:* Histogram of isolation distances for 1,647 lateral septal neurons. *Lower:* Histogram of peak waveform amplitudes for 1,647 lateral septal neurons. **(D)** *Upper:* Histogram of isolation distances for 2,297 CA1 neurons. *Lower:* Histogram of peak waveform amplitudes for 2,297 CA1 neurons. **(E)** *Upper:* Histogram of isolation distances for 654 CA3 neurons. *Lower:* Histogram of peak waveform amplitudes for 654 CA3 neurons. **(F)** Average velocity plots for the circle alternation (N=2,889 trials), central alternation (N=6,608 trials), and linear (N=625 trials) tracks. Bounds are +/- one standard deviation. **(G)** Histograms of all translational velocities across the entire duration of all trials for each behavior type. **(H)** Histograms of all trial durations for each behavior type. **(I)** Behavioral tracking data for the three trial types; central stem alternation (left), linear track (center), and circle maze alternation (right). Green and red dots indicate the start and stop locations for individual trials. **(J)** Population average firing rates (y-axis) for lateral septum (magenta) and hippocampus (black) across all positions (x-axis). Bounds are +/- 3 SEM.

Figure S2. Firing rate and firing phase are independent variables at the single trial level. Related to Figures 1 and 2. **(A)** *Upper:* For the example neuron in Figure 1A-C, the circular-linear correlation between CA1 theta phase and instantaneous firing rate is plotted (black) for each trial (N=21; X-axis). The mean of a null distribution (circularly shifted data with random offsets; N=100 shuffle) is plotted in blue with bounds that represent ± 1 standard deviation from the mean. *Lower:* For each trial the P-value when comparing these values is plotted as the black line. The red line indications P=.05. **(B)** For every action potential for the example neuron in Figure 1a-c, the instantaneous firing rate was calculated (1 /

$[ISI_{pre}+ISI_{post}]/2)$. This instantaneous firing rate (y-axis) is plotted relative to the CA1 theta phase (x-axis) at which the action potentials occurred. Note reduced rate at the peak of the theta cycle (0). **(C)** For all CA1/CA3 conditions the mean (across trials) circular linear correlation for actual data (x-axis) is plotted against the mean circular linear correlation taken from the circular shifted null distribution (y-axis). Red: Neurons with significantly ($P<.05$) higher actual correlations, when compared to the null distribution. They account for less than 2% of all conditions. **(D)** Histograms for all CA1/CA3 conditions shown in Fig. S2C. Blue shows the actual data, red shows the shuffled data. The black and red lines indicate the means of the distributions for actual and shuffled data, respectively. **(E** and **F)** Same as **C** and **D** for all LS conditions.

Figure S3. Lateral septum is a major target of the hippocampal formation. Related to Figures 3-7. **(A)** 55 CA1/CA3 injections were downloaded from the Allen Institute mouse connectivity atlas. For each injection, 9 target regions were selected (lateral septum, subiculum, entorhinal, retrosplenial, orbitofrontal, prelimbic, infralimbic, posterior parietal, and primary visual cortices). For each target region, the normalized fluorescence intensity (y-axis; log-scale) is plotted for each injection (x-axis). Injections are sorted by total injection volume. **(B)** Histograms showing the log-scaled fluorescence intensity across all 55 injections, for each target region. Values given in the upper right corner of each plot are the median value across all 55 injections. **(C)** Our own experiments: Upper images are brain slices from a red retrobead injection (Lumaflour; 100 nL) into the lateral septum of a Long-Evans rat. Below are slices of the hippocampal formation, showing retrobead filled pyramidal neurons in both the CA1 and CA3 regions of the hippocampus.

Figure S4. LS phase coding examples. Related to Figure 3. *Left Column:* Six example hippocampal place cells. Grey dots indicate position tracking data, colored dots indicate the firing of an action potentials at that position. The color indicates the mean firing phase, relative to LFP theta recorded in the CA1 pyramidal layer, for each action potential. Peak = positive. Mean firing phase is calculated for each action potential as the circular mean of the ten closest (in position) action potentials. *Columns 2-5:* 21 example LS neurons. White arrows indicate the start position and direction of travel for each neuron.

Figure S5. Gamma assembly strength is independent from phase locking. Related to Figure 5. **(A)** Diagram of assembly strength quantification. Multiple predictors (theta phase, velocity, position, and a temporally smoothed peer spike train) were given to a generalized linear model. Model deviances of fit were taken for different temporal smoothing windows (1-150 ms) and compared against each other and a shuffled control (red line; bounds are ±3 STD). **(B)** Assembly strength is independent from HPC theta phase kappa values **(C)** Assembly strength is weakly negatively correlated with theta phase resultant vector of HPC neurons **(D)** Optimal smoothing timescale is independent from HPC theta phase kappa values **(E)** Optimal smoothing timescale is weakly positively correlated with HPC theta phase resultant magnitudes.

Figure S6. Lateral septal phase code can be anchored to distal and local cues. Related to Figure 2. **(A)** Example neuron recorded in seven different rotation conditions which is anchored to distal cues. *Top row:* Behavioral tracking data. *Bottom row:* Position-phase scatter plots of all action potentials recorded for that behavioral condition. Magenta lines highlight the 'phase-field' for each condition. **(B)** Example neuron recorded in seven different rotation conditions that is anchored to local cues. **(C)** Circular standard deviations are plotted against position (all spikes within +/- 20 bins), and circularly shifted to be aligned across conditions relative to the goal location (left column) or allocentric room cues (right column). Bold line is the mean, bounds are ± one standard deviation. Cell #44 precession better aligns across conditions relative to allocentric cues, while cell #13 precession better aligns relative to the goal location. **(D)** Reference frame data (x/y position, route position, distance to the goal, or acceleration/velocity variables) were used to predict the firing phase of LS neurons. Comparison is a two-sample T-test, * is $p < 10^{-10}$.

Figure S7. Bayesian ensemble decoding of position using firing rates or firing phases. Related to Figures 2-3. **(A)** Density heatmap of 12,078 HPC ensembles (1-83 cells) that used firing phases to decode position. Y-axis is the mean squared error for each model, X-axis is the number of HPC neurons in the ensemble, and the color axis is model counts. Colored lines are the best polynomial fits with order = 2. **(B)** Density heatmap of 12,078 HPC

ensembles (1-83 cells) that used firing rates to decode position **(C)** Density heatmap of 11,026 LS ensembles (1-53 cells) that used firing phases to decode position **(D)** Density heatmap of 11,026 LS ensembles (1-53 cells) that used firing rates to decode position. **(E)** Overlay of polynomial fits for different regions (LS/HPC, magenta/black) and coding types (phase/rate, dashed/solid). **(F)** Estimated number of neurons necessary to reduce the mean squared error to < 100 (~15 centimeters). The polynomial fits for each decoder type (LS phase, LS rate, HPC phase, and HPC rate) are interpolated until a MSE value of less than 100 (~15 cm) is obtained.

Supplemental Figure 1

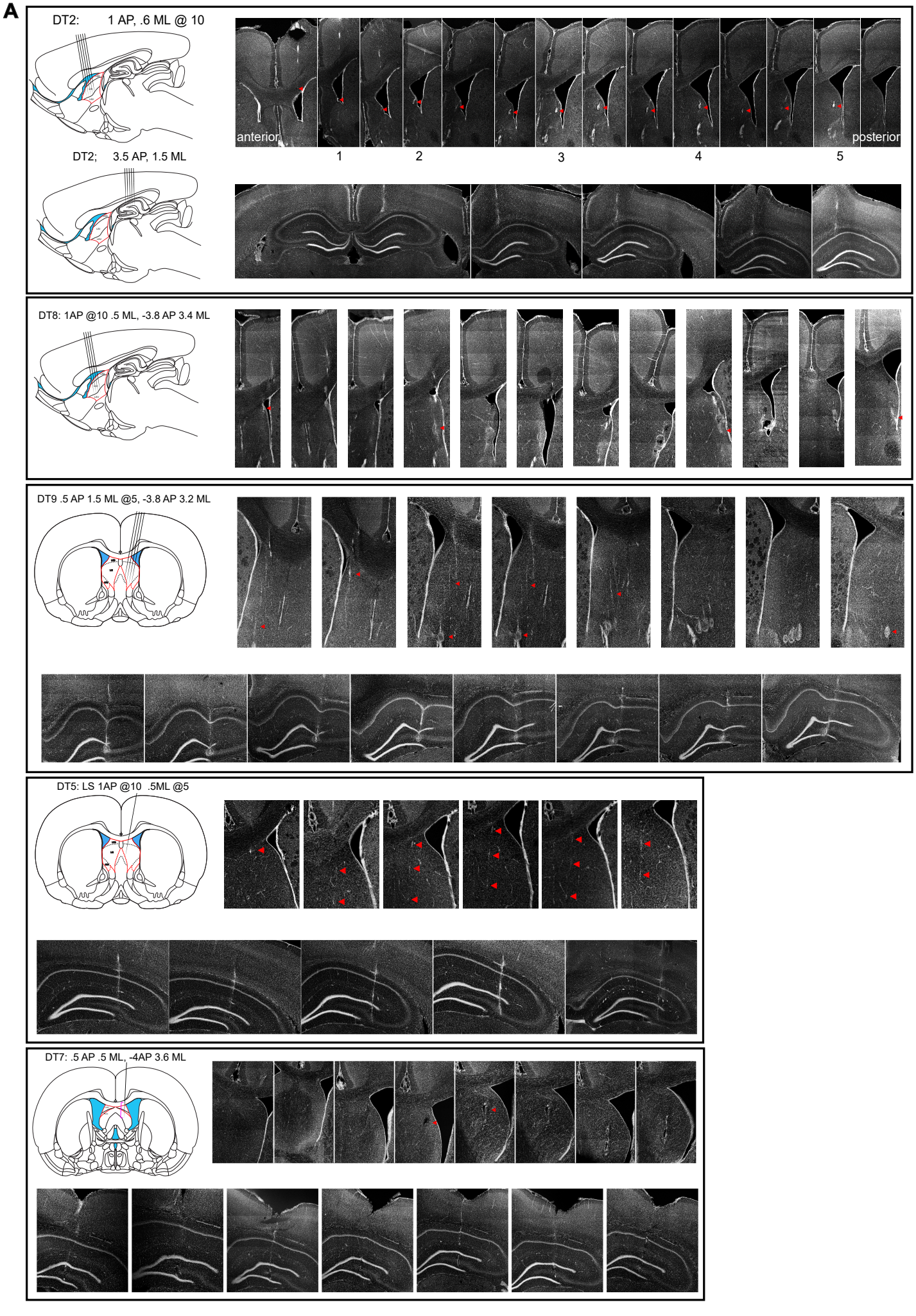

Supplemental Figure 1

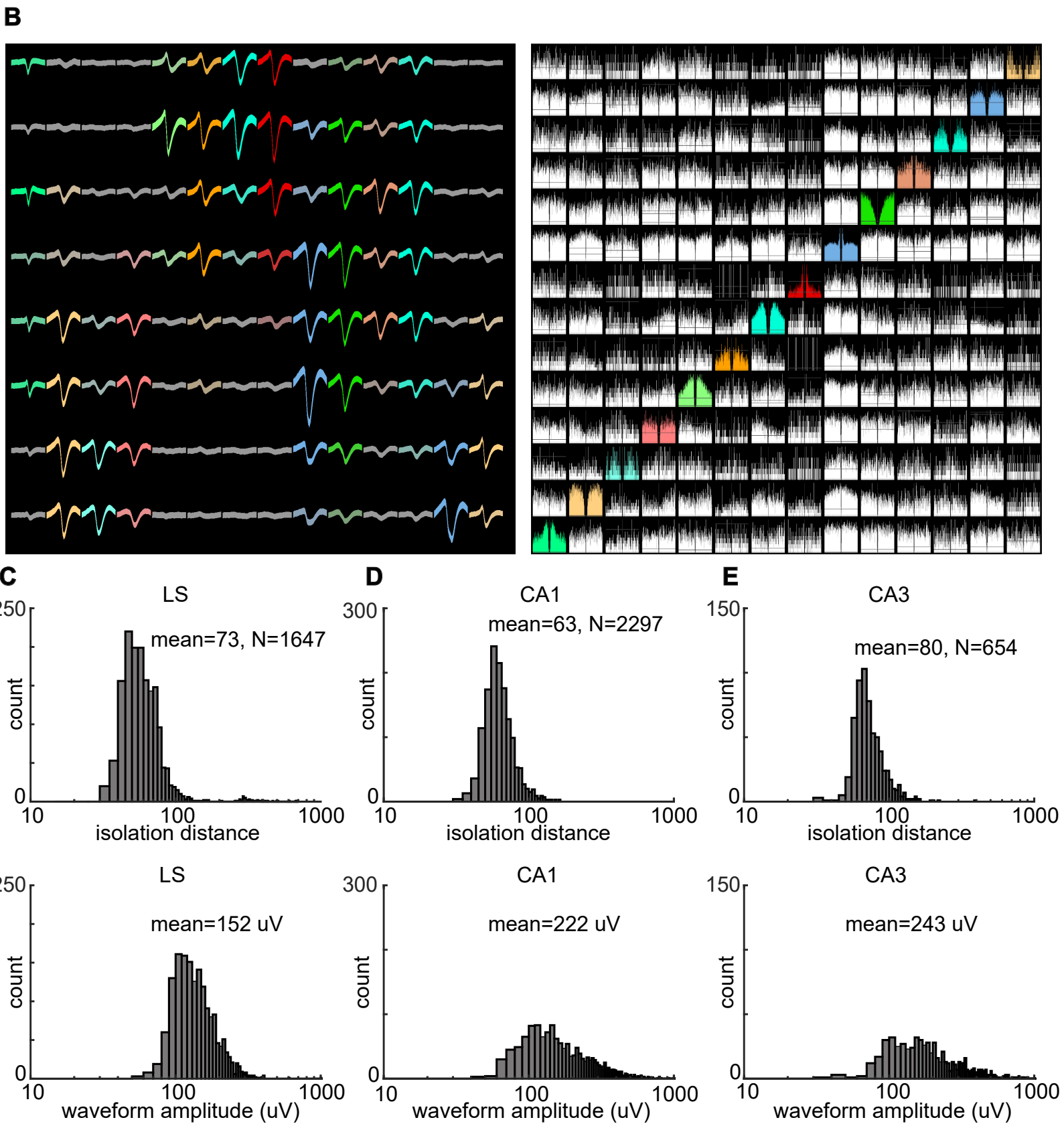

Supplemental Figure 1

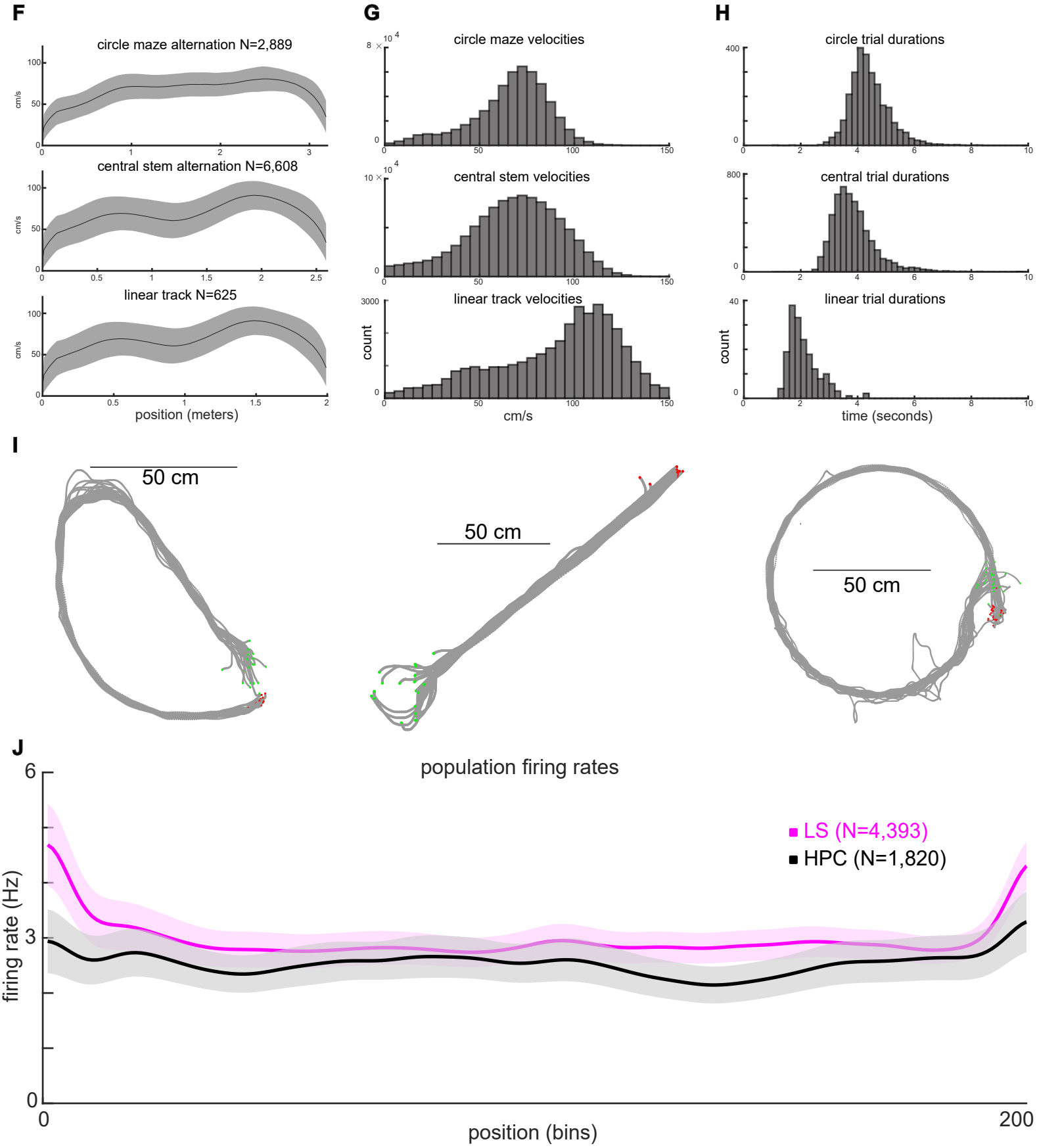

Supplemental Figure 2

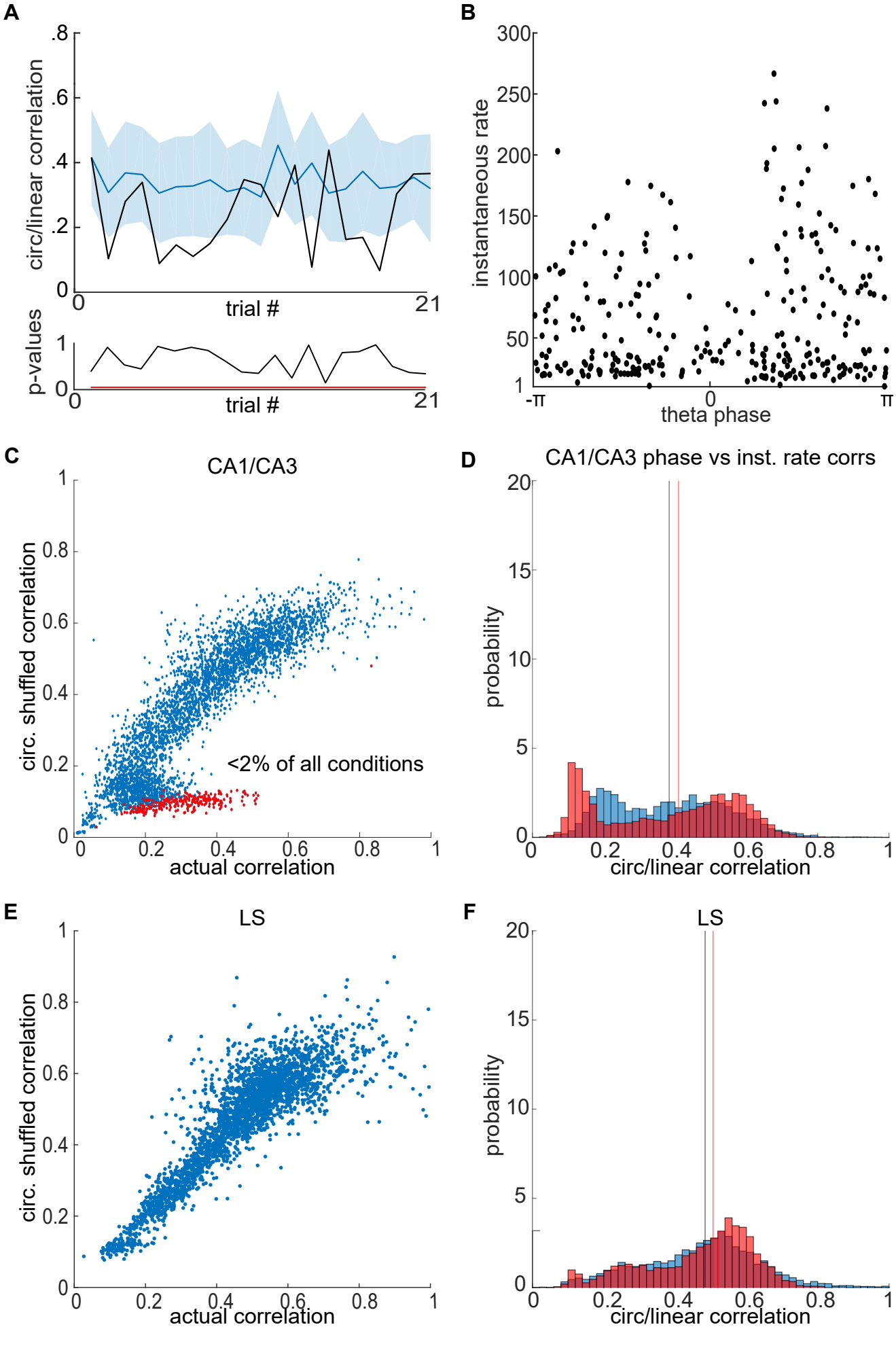

Supplemental Figure 3

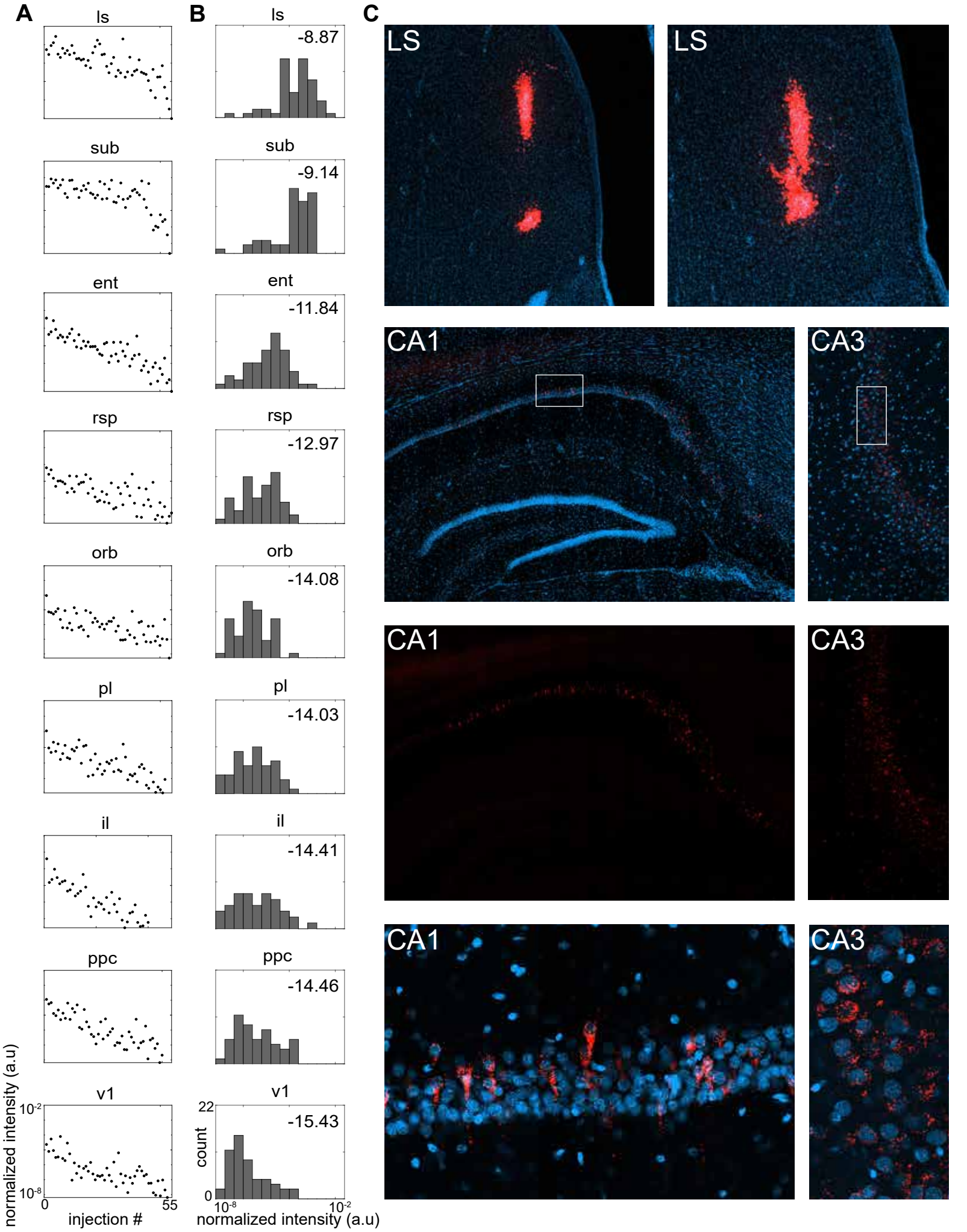

Supplemental Figure 4

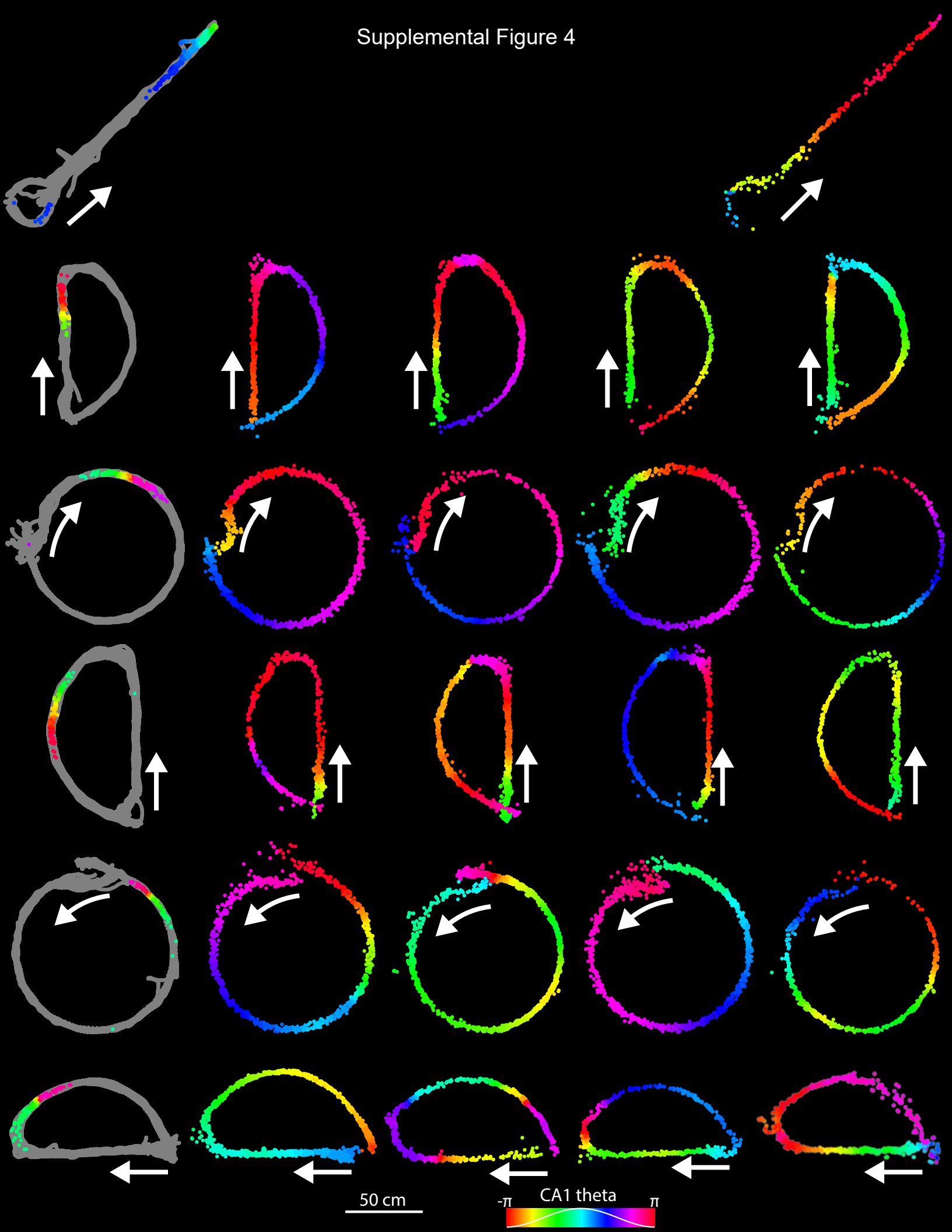

Supplemental Figure 5

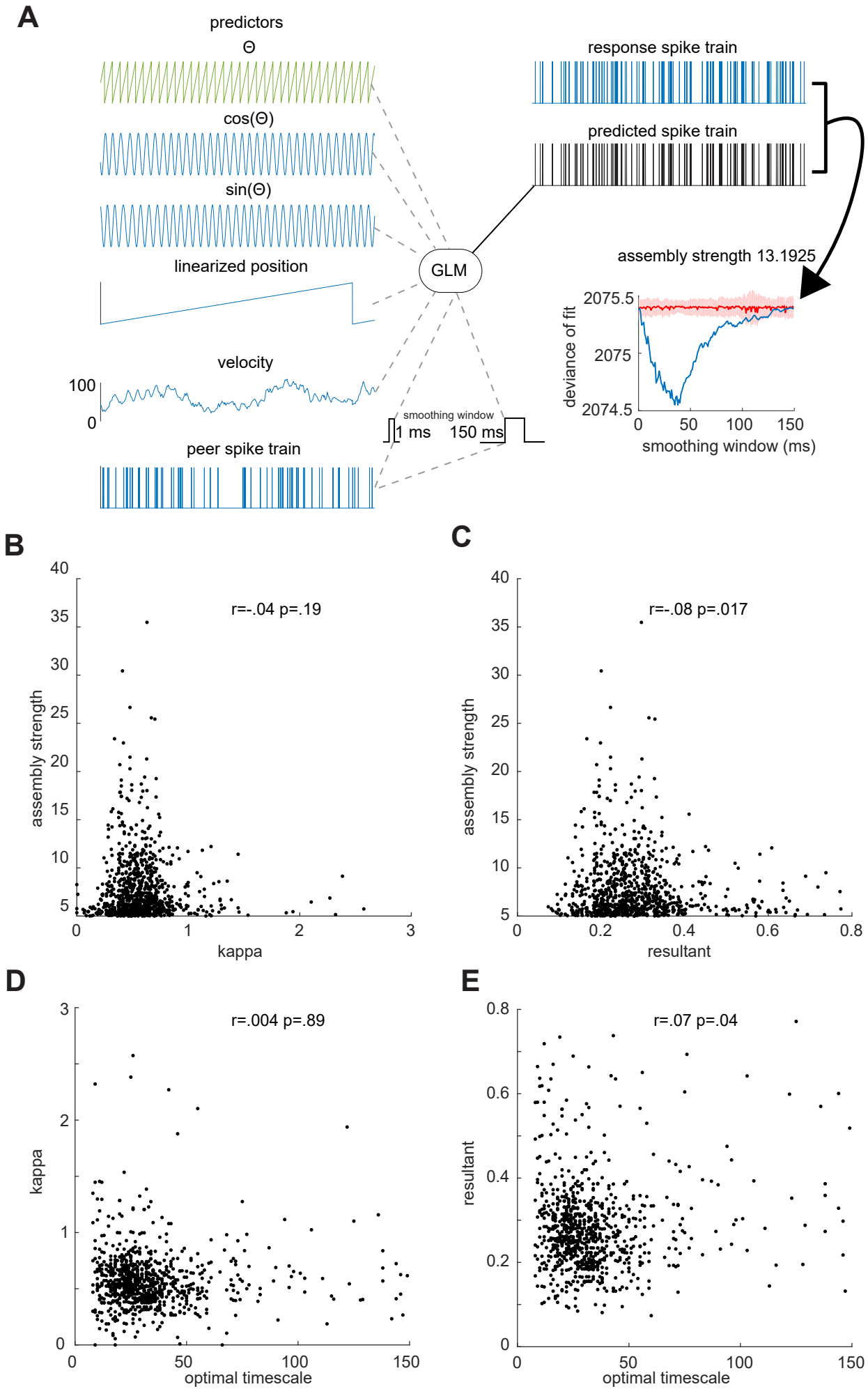

Supplemental Figure 6

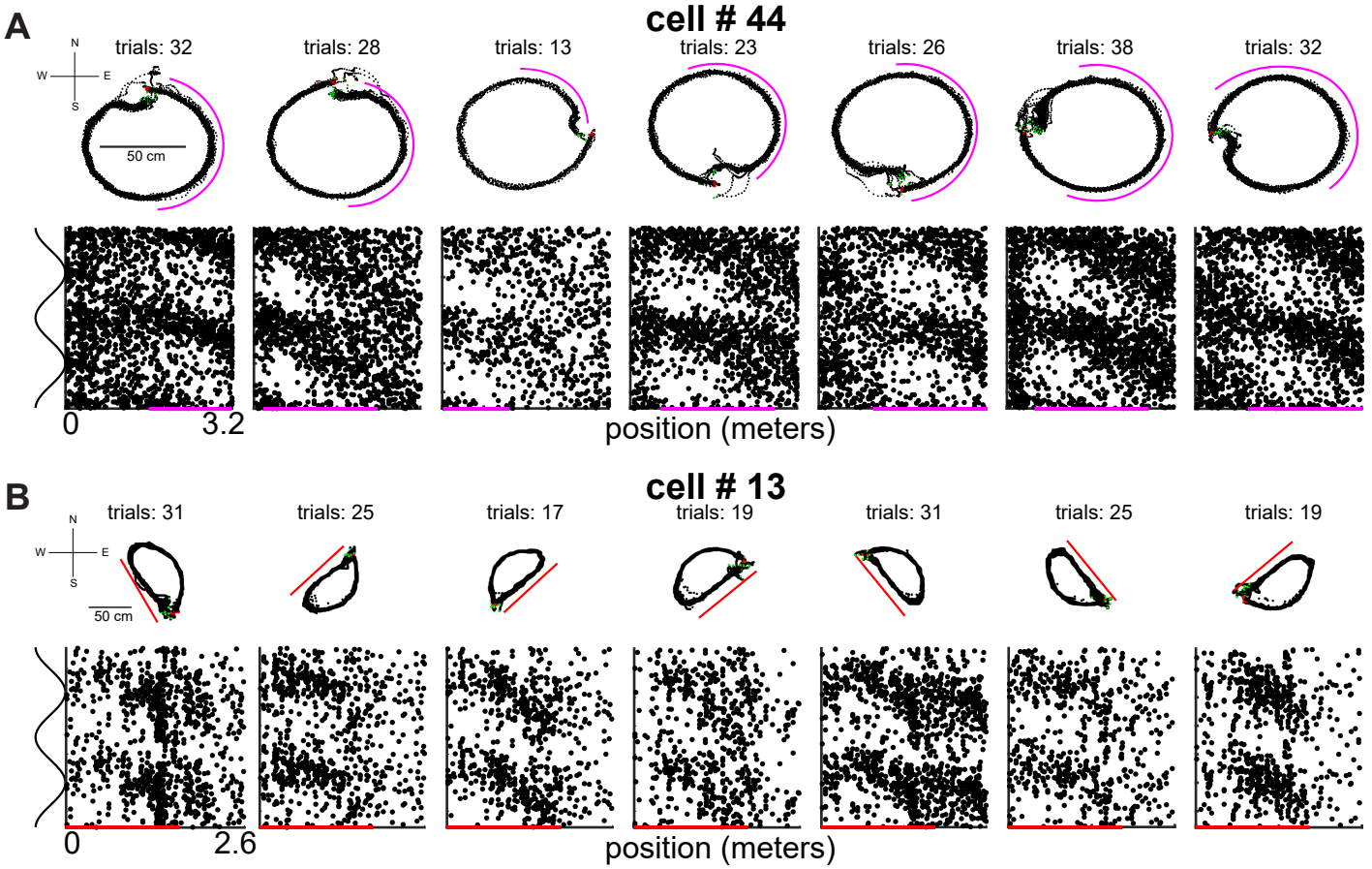

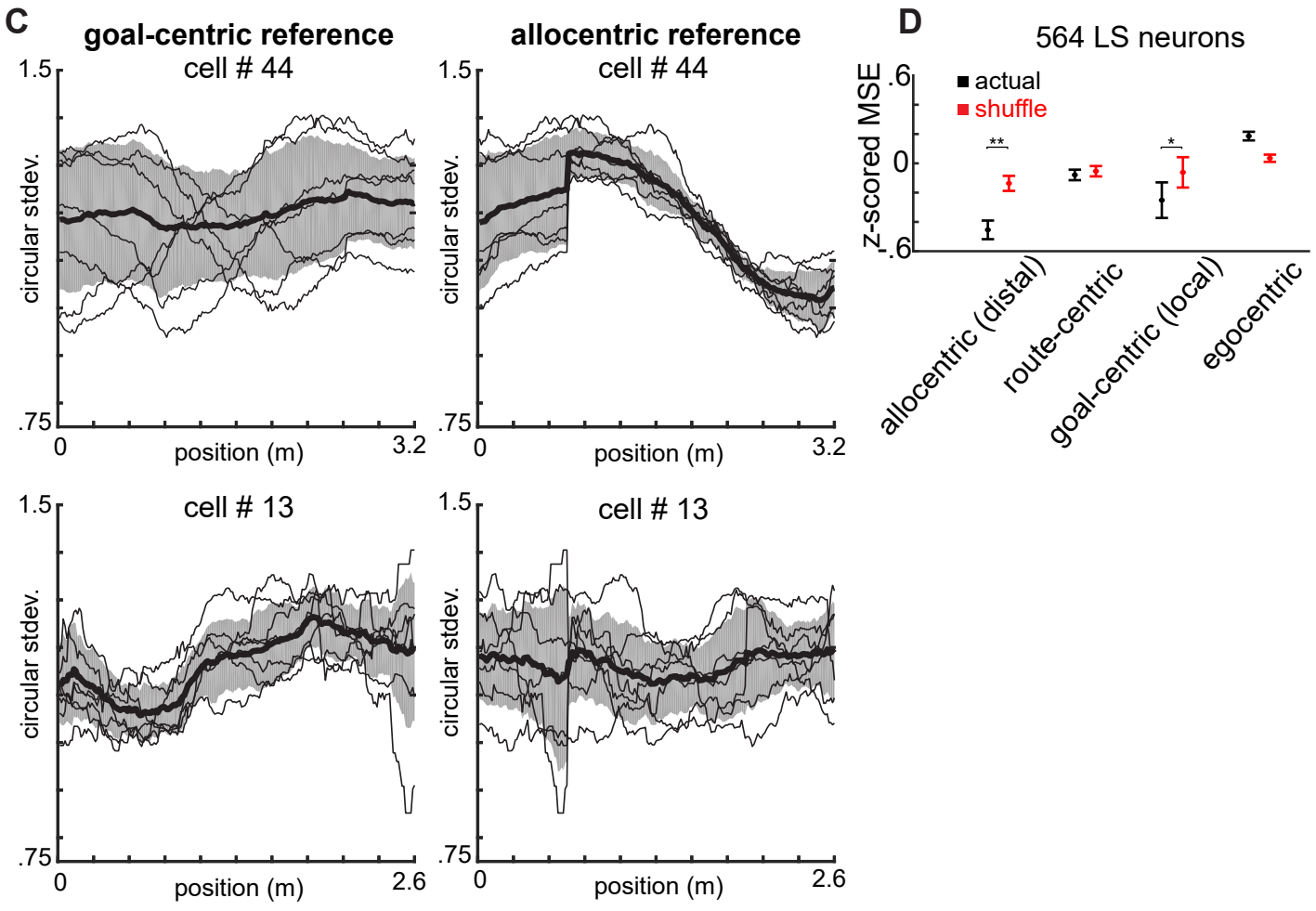

Supplemental Figure 7